

# An equivalent circuit model of a rectangular bracket shaped DGS and its microwave filter applications

Baidenger Agyekum Twumasi<sup>\*,\*\*</sup>, Jia-Lin Li<sup>\*</sup>

A lumped- $LC$  equivalent circuit to model a novel rectangular bracket shaped defected ground structure (DGS) is presented in this paper. The presented equivalent circuit can accurately predicate the frequency responses, in terms of the magnitude and phase responses of  $S$  parameters, of the studied DGS. The lumped  $LC$  parameters of the presented model are extracted based on a unit cell of the DGS. Further, the model is found to be applicable in microwave engineering, including microwave filter designs. Some design examples are presented and examined. The studied DGS based microwave filters characterize maximum passband flatness, sharp skirt between the passband and stopband and wide stopband. The studied equivalent circuit model can accurately predicate the frequency responses including the magnitude and phase of  $S$  parameters.

**Keywords:** defected ground structure, lumped element, microstrip periodic structure, microwave filter

## 1 Introduction

The defected ground structure (DGS), first given the term by Korean scientist Y.-C. Joeng in 2003 for power amplifier applications [1], is realized by periodically etching off defected patterns on the metallic ground plane. It is the same with the photonic bandgap (PBG) and electromagnetic bandgap (EBG) in principle, thus being widely exploited in application to optical and microwave engineering. The reason is attributed to the bandgap, slow-wave and negative index refraction characteristics. This makes it attractive for circuits, components and systems with performance improvement, compact realization and so on. The typical potential applications in microwave engineering involve directional couplers [2], power dividers [3], antennas and arrays [4–10] and of course, the microwave filters [11–22]. However, the patterned ground or DGS is a special structure that cannot be found from the classic microwave circuit models.

The popular solutions are based on full-wave electromagnetic (EM) simulations. However, the EM based designs/simulations of such an array of DGS are time consuming, especially for a large number of DGS unit cells. Thus, an accurate equivalent circuit model that can exactly predicate the DGS performance (in terms of transmission, reflection, delay, *etc*) is highly desirable to improve the design efficiency and further push towards applications in engineering. To date, studies on modeling some types of DGS have been reported, but in general, each model is only suitable for its related special case due to the complexity and variation of the DGS. Meanwhile, for most models, the accuracy needs to be improved.

In this paper, a novel microstrip periodic structure is produced by etching the resonant element on the ground

plane to form a rectangular bracket shaped DGS, and its associated lumped- $LC$  equivalent circuit model are studied. The lumped- $LC$  parameters are extracted from EM numerical calculations corresponding to a unit cell of the proposed DGS. Advantages of the studied DGS include maximum passband flatness, sharp skirt between the passband and stopband, and wide stopband, thus making it attractive for potential applications in microwave engineering, such as microwave filter designs. Based on the presented unit cell, high selectivity microwave filters are developed and implemented. Meanwhile, the studied equivalent circuit model can accurately predicate the frequency responses in terms of the magnitude and phase of  $S$  parameters. The design and demonstration of prototype filters, by cascading unit cells of the proposed DGS, are presented. Results from both EM numerical calculations and equivalent circuit evaluations as well as experimental examinations validate the analyses and discussions.

## 2 Unit cell of the proposed DGS and its performance

A unit cell of the proposed DGS is shown in Fig. 1(a). One can see that the unit cell is composed of rectangular bracket shaped pattern that is etched off on the metallic ground plane, namely the backside of a microstrip transmission line (characteristic impedance  $Z$ ). The proposed structure can effectively distract the shield current distribution on the ground, thus changing the microstrip-line parameters such as the equivalent inductance  $L$  and capacitance  $C$ . Moreover, with this structure, the basic resonant element can exhibit elliptic function responses. To

\* School of Physics, University of Electronic Science and Technology of China, Chengdu 610054, China, jialinli@uestc.edu.cn, \*\* Ho Technical University (HTU), Ho, Ghana, btwumasi@htu.edu.gh,

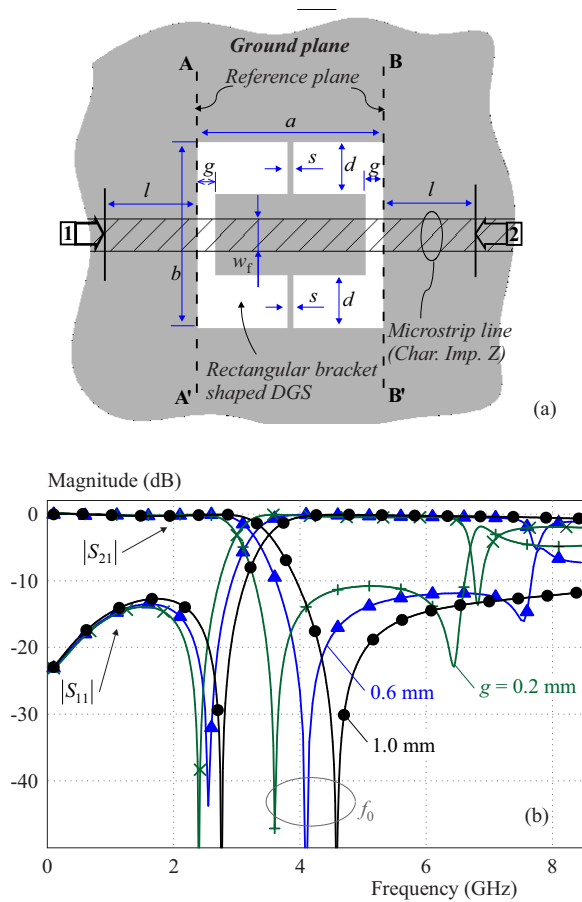


Fig. 1. (a) – layout of the proposed DGS unit, (b) – simulated frequency responses against some values of  $g$

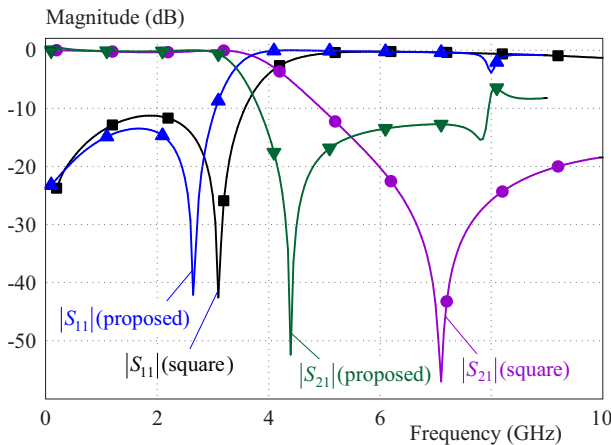


Fig. 2. Frequency responses from EM simulations for a unit cell of the rectangular bracket shaped and the square shaped DGSs, dimensions and the substrate of the square DGS are the same with the report in [10]

validate the proposed DGS pattern, the unit cell is numerically characterized based on full-wave EM simulations. Here, the substrate utilized has a relative permittivity of  $\epsilon_r = 9.6$  and a thickness of  $h = 0.8$  mm. Dimensions of a unit cell are (units: mm):  $a = 7$ ,  $b = 7$ ,  $d = 2$ ,  $g = 0.7$ ,  $s = 0.2$  and  $w_f = 1.2$ . The EM simulations show a fundamental resonance,  $f_0$ , of approximately 4.4 GHz.

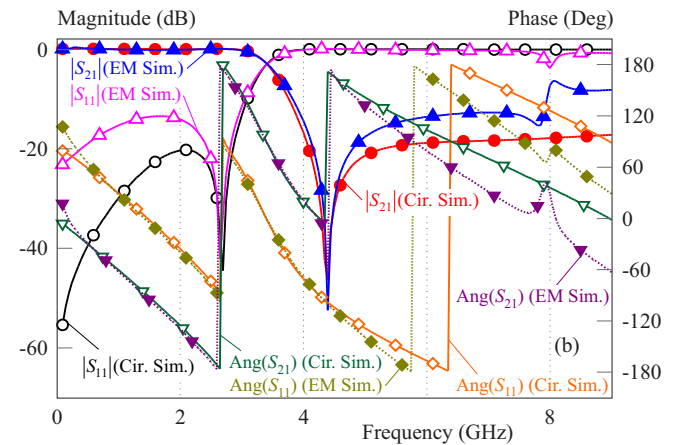
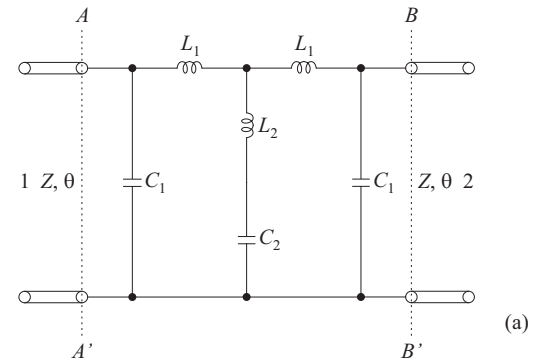
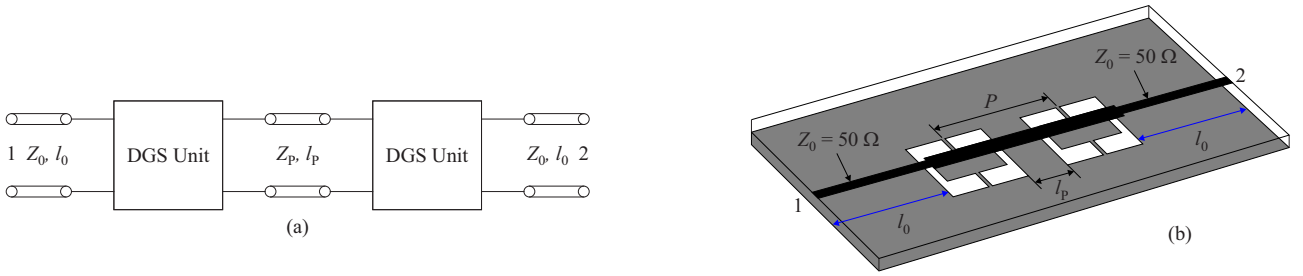


Fig. 3. (a) – equivalent LC circuit model of the proposed DGS, (b) –  $S$  parameters from full-wave EM calculations and equivalent circuit evaluations

The numerically calculated frequency responses are shown in Fig. 1(b), where a variation of the parameter  $g$  for several values is presented for performance comparisons. It can be seen from Fig. 1(b) that as  $g$  increases, the resonance shifts to higher frequencies while the bandwidth is increased. Based on the responses, the resonance and bandwidth can be controlled by properly selecting the dimensional parameters of the proposed rectangular bracket shaped DGS. To further show the performance of the studied structure, frequency responses of a unit cell of square shaped DGS with  $a = b = 7$  mm and a square DGS reported in [10] for  $W/L = 1$  are evaluated as illustrated in Fig. 2. The results show the proposed DGS can exhibit sharp skirt between the passband and stopband, and the square DGS in [10] can be treated as a special case of the studied DGS here.

### 3 Equivalent LC model of a unit cell of the proposed DGS

In order to examine the DGS pattern, an equivalent model is presented as shown in Fig. 3(a). In this model,  $L_1$  and  $C_1$  denote the inductance and capacitance of each DGS region. Meanwhile, the equivalent  $L_2$  and  $C_2$ , resulting from the high-low-high impedance transmission



**Fig. 4.** (a) – schematic transmission-line model by cascading two unit cells, (b) – the corresponding 3-D layout

line within the pair of brackets, formulates the enhanced resonance of the proposed DGS. With this pattern, the current path on the ground can be effectively disturbed, generating the in-band reflection pole and out-of-band transmission zero, thus improving the response. For the proposed pattern, the in-band reflection pole primarily results from the resonance of the extra high-low-high transmission line that is modeled as  $L_2$  and  $C_2$  in series. Meanwhile, the out-of-band transmission zero is due to the resonance of the basic square hole denoted as  $a \times b = 7 \times 7 \text{ mm}^2$ , which is modeled as a  $\pi$ -shaped network consisting of  $L_1$  and  $C_1$ , as shown in Fig. 3(a). Notice that in this study, it is assumed that the transmission line and the substrate are lossless.

Now, to find the equivalent network parameters, the  $S$  parameters of a DGS unit cell at the reference plane are calculated using EM simulator (Ensemble from Ansoft). To validate the proposed equivalent model, a DGS unit cell shown in Fig. 1(a) was simulated. By extracting the values of lumped  $LC$  elements, the equivalent network parameters are:  $L_1 = 2.4701 \text{ nH}$ ,  $C_1 = 0.0785 \text{ pF}$ ,  $L_2 = 1.4226 \text{ nH}$ ,  $C_2 = 0.9281 \text{ pF}$ , where the extraction refers to  $w_f = 1.2 \text{ mm}$ , corresponding to a characteristic impedance  $Z = 40 \Omega$  of the microstrip line. The magnitude and phase of  $S$  parameters from EM simulations as well as the equivalent circuit evaluations are presented in Fig. 3(b). It can be seen that the results from equivalent  $LC$  evaluations match the ones of EM calculations.

#### 4 Two cascaded DGS unit cells for microwave filter application

Based on the above developed equivalent circuit model, one needs to further consider the following issues in practice: the system impedance reference, the mutual coupling and the separation between adjacent unit cells. By checking the  $LC$  model in Fig. 3(a), it is found that the former two can be associated with, thus primarily determined by, the equivalent capacitance  $C_1$ . The separation, or the interval, between adjacent unit cells is referred to the Richard transformation and Kuroda identity in classic microwave engineering, thus it is set to a one-eighth wavelength. Therefore, the value of model parameter  $C_1$  given in Section 3 is to be modified.

Considering two DGS unit cells cascaded with an interval of  $l_P$ , and the system impedance of the input-

and output-ports are referred to  $Z_0$ , the corresponding schematic transmission-line model is shown in Fig. 4(a), and the 3-D layout is shown in Fig. 4(b). The correction of  $C_1$  is based on the following procedure:

**Step 1:** Initializations. Each unit cell of the studied DGS was formulated by its lumped  $LC$  parameters, and the values were initially set as those corresponding to a unit cell extracted in Section 3. The interval  $l_P$  is set to a one-eighth wavelength at the resonance. Meanwhile, the input and output were set to the system impedance  $Z_0$ ; the reference distance  $l_0$  between the port and the cell is greater than that of a quarter-wavelength at the fundamental resonance,  $f_0$ .

**Step 2:** Circuit optimizations based on the schematic transmission-line model. The optimization in this step is to maintain a close resonance related to the unit cell, and to have acceptable input and output matching. The primary focuses are to correct the equivalent capacitance  $C_1$  that accounts for the step discontinuity of the transmission line and also formulates the coupling effects between adjacent unit cells.

**Step 3:** Full-wave EM validations. Based on the initially determined interval  $l_P$  to construct the 3-D layout and perform the EM field simulations and further comparing the EM results with the equivalent circuit evaluations, thus verifying the effectiveness of the model parameters. The final work is to slightly tune the parameter values to present matched responses between EM and equivalent circuit simulations.

Based on Step 1, the width of the  $50\text{-}\Omega$  line for such a kind of substrate is  $0.7 \text{ mm}$  with its length  $l_0 = 10 \text{ mm}$ . The initial interval  $l_P$  is estimated based on the following calculations

$$\varepsilon_e = \frac{\varepsilon_r + 1}{2} + \frac{\varepsilon_r - 1}{2} \sqrt{1 + 12 \frac{W}{h}}, \quad (1)$$

$$\lambda_g = \frac{c_0}{f_0 \sqrt{\varepsilon_e}} \quad (2)$$

where  $c_0$  is the light speed in free space and  $f_0$  is the resonance.

For the utilized substrate,  $\varepsilon_r = 9.6$  and  $h = 0.8 \text{ mm}$ , and here  $W = 1.2 \text{ mm}$ , thus the effective relative permittivity  $\varepsilon_e = 6.733$  from (1), and further  $\lambda_g = 26.27 \text{ mm}$  from (2). Hence,  $l_P = \lambda_g/8 = 3.28 \text{ mm}$ .

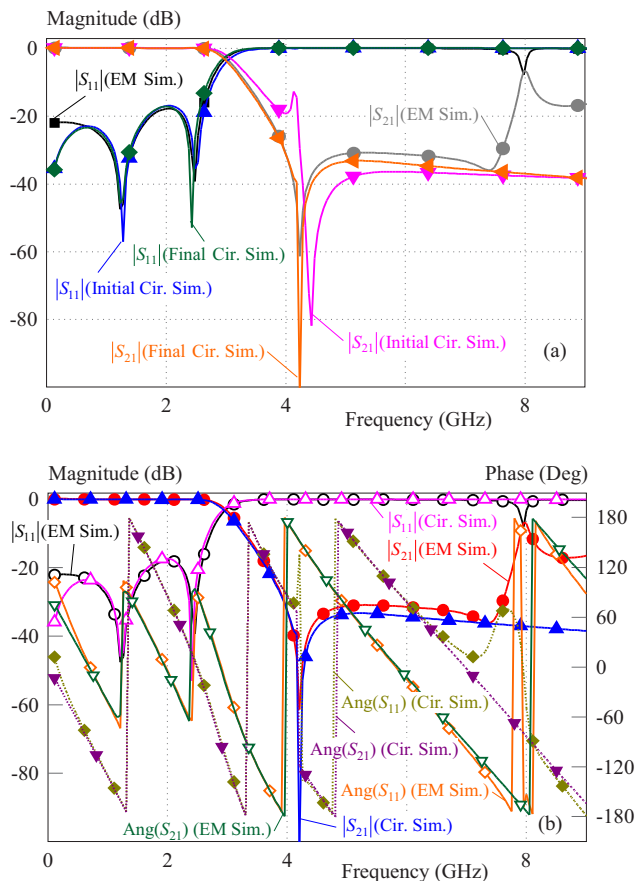


**Fig. 5.** (a) –  $S$  parameters from EM calculations and equivalent circuit evaluations for fig. 4, (b) – magnitude and phase responses of  $S$  parameters from EM simulations and final circuit simulations

From Step 2, the optimized  $C_1$  of the two cascaded unit cells are 0.2756 pF. Further, from Step 3, the numeric EM calculations are performed, where the interval  $l_P$  is also optimized to achieve a suitable mutual coupling, and it is 3.03 mm after EM optimizations. Figure 5 records the simulated results. It is seen that the responses from EM evaluations and the circuit calculations based on Step 2 (represented as the initial circuit simulation in Fig. 5(a)) are consistent, except the small deviation of the resonance. To correct this deviation, a slightly fine-tuning of the equivalent  $LC$  parameter values was carried-out.

Figure 5 shows the recorded results for comparisons. It is seen that after slight tuning the values of the  $LC$  parameters, the performances between the final circuit simulations and the EM results were in good agreement either for the transmission or for the reflection responses. Notice that an extra resonance at approximately 8 GHz from EM simulations is due to the spurious resonance. In this contribution, the developed  $LC$  network is dedicated to modeling the in-band (or passband) and near in-band responses and therefore, it does not involve the spurious response. But in general, the studied  $LC$  network and its related parameter values can effectively predicate the EM responses with a high accuracy.

Correspondingly, as compared to the values in Step 2 with  $L_1 = 2.4701$  nH,  $C_1 = 0.2756$  pF,  $L_2 = 1.4226$  nH,

$C_2 = 0.9281$  pF, the final  $LC$  parameter values are slightly changed to  $L_1 = 2.4434$  nH,  $C_1 = 0.2612$  pF,  $L_2 = 1.4856$  nH, and  $C_2 = 0.9674$  pF from Step 3. These results correspond to relative errors of 1.09% for  $L_1$ , 1.68% for  $C_1$ , 4.24% for  $L_2$  and 4.06% for  $C_2$ , respectively, where the relative error is calculated as

$$RE = \frac{|\mathcal{F}_{i\_ini} - \mathcal{F}_{i\_fin}|}{\mathcal{F}_{i\_fin}} \times 100\% \quad i = 1, 2 \quad (3)$$

where  $\mathcal{F}$  denotes  $L$  or  $C$ , and subscripts  $i\_ini$  and  $i\_fin$  represent the initial and final values of the  $i^{\text{th}}$  element.

Figure 5(b) shows the magnitude and phase performance, where consistent phase responses can also be found between EM and final circuit simulations.

## 5 Cascading more unit cells for application to high-order filters

Based on Section 4 with its final  $LC$  parameter values of two cascaded unit cells, microwave filters can be developed by further cascading more DGS unit cells, thus constituting the periodic structure. Such a cascading is generally necessary in microwave engineering since it can improve the microwave filter performance like increasing the stopband suppression in practice. Here the design procedure is simplified as:

**Step 1:** Check the validity. Based on the  $LC$  parameter values and the periodic interval presented in Section 4, estimating the performance from circuit simulations for the schematic transmission-line model.

**Step 2:** EM validations. For the corresponding 3-D layout, performing EM field simulations, and comparing the EM results with the equivalent circuit evaluations, verifying the effectiveness of the model parameters. Finally, slight tuning the parameter values to give consistent responses between EM and equivalent circuit simulations.

Here, two high-order filters are further developed based on the above procedure. The first one corresponds to cascading three unit cells. Figure 6(a) shows the transmission-line model. The circuit evaluation from Step 1 indicates that the performance is good, as shown in Fig. 6(c), implying the study given in Section 4 being extendable. The 3-D field simulation, from Step 2, illustrates that the studied filter works well, where the corresponding 3-D layout is shown in Fig. 6(b) and the simulated response is presented in Fig. 6(c). Also, a slight difference lies in the resonances and to correct this offset, just slight tuning yields matched responses, as displayed in Fig. 6(c). The final  $LC$  parameter values based on Step 2 were found to be  $L_1 = 2.4034$  nH,  $C_1 = 0.2662$  pF,  $L_2 = 1.5556$  nH, and  $C_2 = 0.9474$  pF.

With the final parameter values, Figure 7 further presents the magnitude and phase responses, both for EM and transmission-line model simulations.

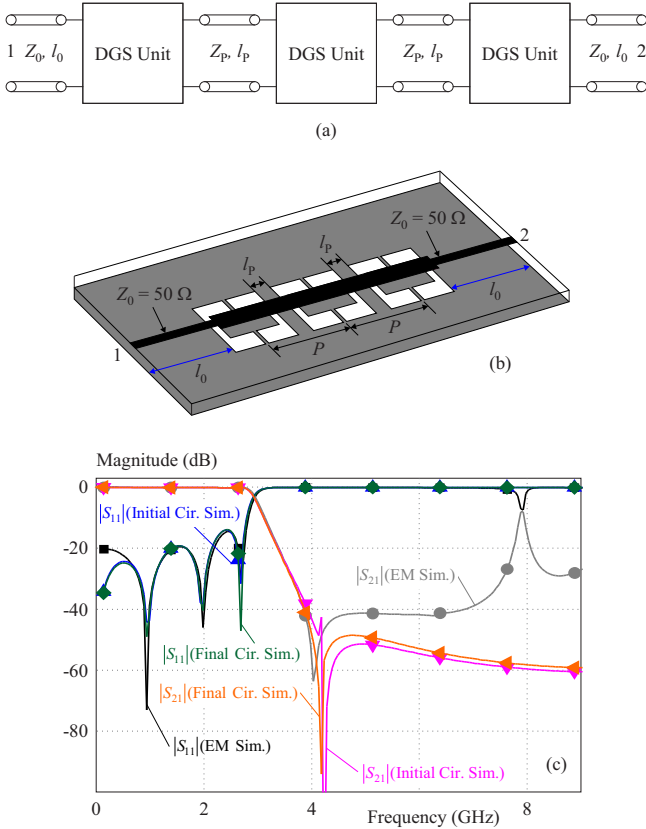


**Fig. 6.** (a) – schematic transmission-line model by cascading three DGS unit cells for microwave filter applications, (b) – the corresponding 3-D layout, (c) –  $S$  parameters from EM and equivalent circuit evaluations

**Table 1.** Final  $LC$  parameter values and relative errors

Cascaded unit cells	$L_1$ (nH)	$C_1$ (pF) (Error in %)	$L_2$ (nH)	$C_2$ (pF) (Error in %)
2	2.4434 (1.24)	0.2612 (0.31)	1.4856 (1.73)	0.9674 (1.37)
3	2.4034 (0.41)	0.2662 (2.23)	1.5556 (2.90)	0.9474 (0.72)
4	2.3934 (0.83)	0.2537 (2.57)	1.4943 (1.16)	0.9481 (0.65)

One can see from the figure that the transmission-line model can precisely predicate the in-band and near in-band responses compared to the EM results.

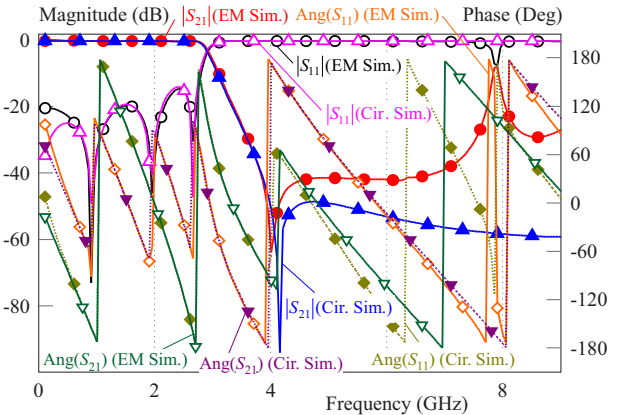
The second demonstrator was developed by cascading four DGS unit cells. Following the above two-step design procedure, the results were found and, for brevity, both the transmission-line model and the 3-D layout are not figured here in this case. Figure 8 describes the performance (including the magnitude and phase responses) from full-wave EM simulations and equivalent circuit calculations, where the final lumped  $LC$  parameter values are  $L_1 = 2.3934$  nH,  $C_1 = 0.2537$  pF,  $L_2 = 1.4943$  nH, and  $C_2 = 0.9481$  pF.

Table 1 lists the final  $LC$  values of the above designed filters, where the error can be treated as the general error and is given by

$$GE = \left| \frac{\mathcal{F}_{i,j\text{cell}} - \frac{\mathcal{F}_{i,2\text{cell}} + \mathcal{F}_{i,3\text{cell}} + \mathcal{F}_{i,4\text{cell}}}{3}}{\mathcal{F}_{i,j\text{cell}}} \right| \times 100\%, \quad (4)$$

$$i = 1, 2 \text{ and } j = 2, 3, 4$$

where  $\mathcal{F}$  denotes  $L$  or  $C$ , and subscript  $j$  in the  $\mathcal{F}_{i,j\text{cell}}$  means the number of cascaded unit cells.



**Fig. 7.** Magnitude and phase responses of  $S$  parameters from EM and final circuit simulations for fig. 6

It is seen that for each case, the  $LC$  values exhibit small errors (less than 3%). These results clearly indicate that the presented equivalent circuit model works well for the proposed rectangular bracket shaped DGS, and further, it can be applicable to high-order microwave filters.

It should be noted there are some studies that presented the equivalent circuit models [11–17], and further extracted the corresponding element values [16, 17]. However in our work, we developed the equivalent model of a unit cell and further by slightly modifying its element parameters, results show the provided model is applicable to high-order microwave filters with good accuracy. To our knowledge, there is no reports from literatures that an equivalent model extracted from a unit cell and further, it can be utilized to design more cascaded cells for microwave filter applications.

## 6 Experimental validations and results

A demonstration microstrip filter by cascading three DGS unit cells was further fabricated on the microwave substrate mentioned above. Fig. 9(a) shows the photograph of the developed filter. The measurement was carried out with an Agilent vector network analyzer, N9918A, with two-port calibrations. Fig. 9(b) presents the measured performance, where for performance comparisons the responses from EM simulations are also involved.

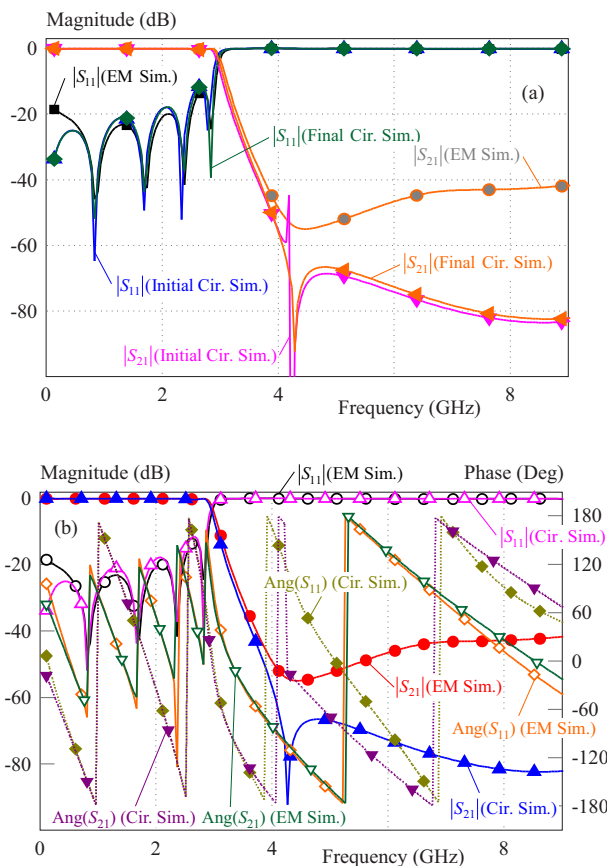


**Fig. 8.** (a) – frequency responses from initial circuit, final circuit and 3-D EM simulations by cascading four unit cells, and (b) – magnitude and phase responses of  $S$  parameters for the final circuit and 3-D EM calculations

It is seen that the measurements match the simulated data reasonably. The measured in-band insertion loss is generally less than 0.3 dB and return loss is better than 13 dB. Three reflection poles can be clearly identified. The out-of-band suppression, from 3.5 to 7.8 GHz, is approximately 33 dB. It is seen there are some offset for the resonance and reflection poles, which could be attributed to the fabrication uncertainties. In general, these results confirmed the study well in this work.

### 7 Conclusions

In this paper, a rectangular bracket shaped DGS for microwave filter applications has been proposed and discussed. An accurate equivalent lumped  $LC$  network has been presented to model the introduced DGS, and further its related  $LC$  parameter values were extracted based on full-wave EM simulations. Microstrip filters with cascaded DGS unit cells can be developed, and the presented model can accurately predicate the frequency response of  $S$  parameters. Results from circuit evaluations, EM simulations and experimental examinations for a fabricated demonstrator validate the study.

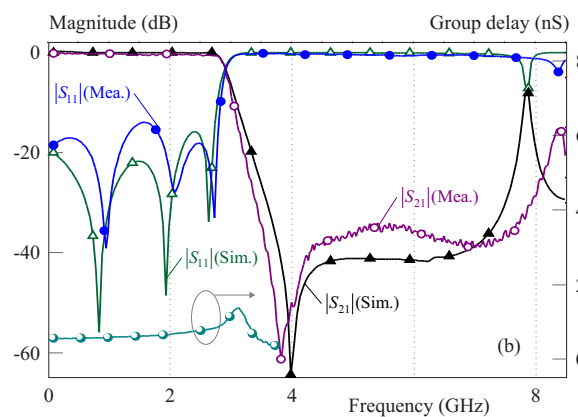
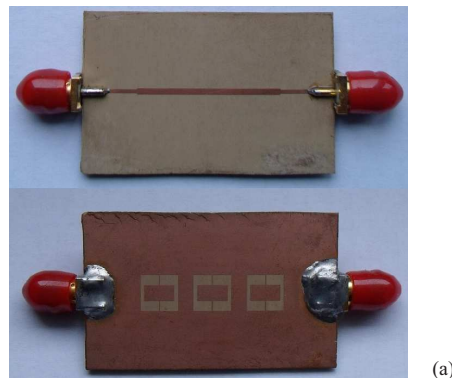


**Fig. 9.** (a) – photographs of the developed microstrip filter by cascading three DGS unit cells, where the upper photo shows the front side and the bottom photo is the back side, and (b) – simulated and measured  $S$  parameters

### REFERENCES

- [1] Y. C. Jeong, S. G. Jeong, J. S. Lim and S. Nam, “A New Method to Suppress Harmonics Using  $\lambda/4$  Bias Line Combined by Defected Ground Structure in Power Amplifiers”, *IEEE Microwave Wireless Components Letters* vol. 13, no. 12, 2003, pp. 538–540.
- [2] V. N. Rachmadini, and A. Munir, “Performance Enhancement of Directional Coupler using Split Ring Resonator”, in *2015 2nd International Conference on Information Technology 2015*, pp. 288–291.
- [3] M. Li, Y. Wu, M. Qu, Q. Li and Y. Liu, “A Novel Power Divider with Ultra-Wideband Harmonics Suppression based on Double-Sided Parallel Spoof Surface Plasmon Polaritons Transmission Line”, *International Journal of RF and Microwave Computer Aided Engineering* vol. 28, no. 4, 2018, pp. 1–7.
- [4] K. Wei, J. Y. Li, L. Wang, R. Xu and Z. J. Xing, “A New Technique to Design Circularly Polarized Microstrip Antenna by Fractal Defected Ground Structure”, *IEEE Transactions on Antennas and Propagation* vol. 65, no. 7, 2017, pp. 3721–3725.
- [5] R. Hussain, M. U. Khan and M. S. Sharawi, “An Integrated Dual MIMO Antenna System with Dual-Function GND-Plane Frequency-Agile Antenna”, *IEEE Antennas Wireless Propagation Letter* vol. 17, no. 1, 2018, pp. 142–145.
- [6] B. R. S. Reddy and D. Vakula, “Compact Zigzag-Shaped-Slit Microstrip Antenna with Circular Defected Ground Structure for Wireless Applications”, *IEEE Antennas Wireless Propagation Letter* vol. 14, 2015, pp. 678–681.

- [7] A. A. Salih, and M. S. Sharawi, "A Dual-Band Highly Miniaturized Patch Antenna", *IEEE Antennas Wireless Propagation Letter* vol. 15, 2016, pp. 1783–1786.
- [8] C. Kumar, M. I. Pasha and D. Guha, "Defected Ground Structure Integrated Microstrip Array Antenna for Improved Radiation Properties", *IEEE Antennas Wireless Propagation Letter* vol. 6, 2017, pp. 310–312.
- [9] B. T. P. Madhav, S. Rajiya, B. P. Nadh and M. S. Kumar, "Frequency Reconfigurable Monopole Antenna with DGS for ISM Band Applications", *Journal of Electrical Engineering* vol. 69, no. 4, 2018, pp. 293–299.
- [10] C. Kumar and D. Guha, "Defected Ground Structure (DGS)-Integrated Rectangular Microstrip Patch for Improved Polarization Purity with Wide Impedance Bandwidth", *IET Microwaves, Antennas and Propagation* vol. 8, no. 8, 2014, pp. 589–596.
- [11] M. Berka, Z. Mahdjoub and M. Hebali, "New Design of Dual-Band Bandpass Microwave Filter based on Electromagnetic Effect of Metamaterial Resonators", *Journal of Electrical Engineering* vol. 69, no. 4, 2018, pp. 311–316.
- [12] A. Boutejdar, A. A. Ibrahim and R. M. Shubair, "A Novel High-Performance DMS/DGS Low-Pass Filter for Radar Applications", in *IEEE International Symposium on Antennas and Propagation* July, 9–14, San Diego, CA, USA, 2017, 2259–2260.
- [13] S. Cao, Y. Han, H. Chen and J. Li, "An Ultra-Wide Stopband LPF using Asymmetric Pi-Shaped Koch Fractal DGS", *IEEE Access* vol. 5, 2017, pp. 27126–27131.
- [14] B. Peng, S. Li, J. Zhu, Q. Zhang, L. Deng, Q. Zeng and Y. Gao, "Compact Quad-Mode Bandpass Filter based on Quad-Mode DGS Resonator", *IEEE Microwave and Wireless Components Letters* vol. 26, no 4, 2016, pp. 234–236.
- [15] S. Sen, T. Moyra and D. Sarkar, "Modelling and Validation of Microwave LPF using Modified Rectangular Split Ring Resonators (SRR) and Defected Structures", *AEU - International Journal of Electronics and Communications* vol. 88, 2018, pp. 1–10.
- [16] U. R. Bhat, K. R. Jha and G. Singh, "Wide Stopband Harmonic Suppressed Low-Pass Filter with Novel DGS", *International Journal of RF and Microwave Computer Aided Engineering* vol. 28, no. 5, 2018, pp. 1–7.
- [17] B. Sahu, S. Singh, M. K. Meshram and S. P. Singh, "Study of Compact Microstrip Lowpass Filter with Improved Performance using Defected Ground Structure", *International Journal of RF and Microwave Computer Aided Engineering* vol. 28, no. 4, 2018, pp. 1–11.
- [18] S. Oh, J. Choi, B. Shin, W. S. Yoon, J. Jeong and J. Lee, "Bandpass Filter Design based on Vertical Split-Ring Resonators", *Electronics Letters* vol. 53, no. 21, 2017, pp. 1412–1414.
- [19] X. K. Gao, H. M. Lee and S. P. Gao, "A Robust Parameter Design of Wide Band DGS Filter for Common-Mode Noise Mitigation in High-Speed Electronics", *IEEE Transactions on Electromagnetic Compatibility* vol. 59, no. 6, 2017, pp. 1735–1740.
- [20] J. Lu, J. Wang and H. Gu, "Design of Compact Balanced Ultra-Wideband Bandpass Filter with Half Mode Dumbbell DGS", *Electronics Letters* vol. 52, no. 9, 2016, pp. 731–732.
- [21] H. Chen, D. Jiang and X. Chen, "Wideband Bandstop Filter using Hybrid Microstrip/CPW-DGS with Via-Hole Connection", *Electronics Letters* vol. 52, no. 17, 2016, pp. 1469–1470.
- [22] A. Barakat, R. Pokharel and T. Kaho, "60 GHz On-Chip Mixed Coupled BPF with H-Shaped Defected Ground Structures", *Electronics Letters* vol. 52, no. 7, 2016, pp. 533–535.

Received 11 December 2018

**Baidenger Agyekum Twumasi** was born in September, 1981 at Nsawam in the Eastern Region of Ghana. He obtained the HND in Elect/Electronic Engineering from Ho Polytechnic in 2004, the Master of Telecommunication Management from HAN University of Applied Sciences in Netherlands in 2011. He is currently a PhD candidate in the University of Electronic Science and Technology of China, majoring in Electronic Science and Technology in the School of Physics. He is a lecturer in Elect/Electronic Engineering at Ho Technical University in Ghana. He is also a graduate student member of IEEE and a member of APS and MTTTS societies. His research interest includes MIMO Antenna Designs, Planar electronic circuits for Telecommunication Applications, Study of Electromagnetic Time Reversal (EMTR) and its Applications, Wireless Power Transfer and its related circuits, Microwave and Millimeter-wave electronic circuits and systems design as well as Telecommunications Management.

**Jia-Lin Li** was born in October 1972 at Sichuan, China. He received the MS degree from the University of Electronic Science and Technology of China (UESTC), Chengdu, China, in 2004, and the PhD degree from the City University of Hong Kong, Hong Kong, in 2009, both in electronic engineering. From September 2005 to August 2006, he was a Research Associate with the Wireless Communication Research Center, City University of Hong Kong, Hong Kong. Since September 2009, he has been with the School of Physical Electronics, UESTC, where he is currently a Professor. His research interests include microwave/millimeter-wave antenna and arrays, circuits and systems, interactions between microwave and complex medium, and so on.